

## Deformation behaviour of steel/SRPP fibre metal laminate characterised by evolution of surface strains

J. Nam<sup>1</sup>, Wesley Cantwell<sup>2</sup>, Raj Das<sup>3</sup>, Adrian Lowe<sup>1</sup>  
and Shankar Kalyanasundaram<sup>\*1</sup>

<sup>1</sup>Research School of Engineering, Australian National University,  
31 North Road, Canberra, ACT 2601, Australia

<sup>2</sup>College of Engineering, University of Liverpool, Brownlow Hill, Liverpool L69 3GJ, United Kingdom

<sup>3</sup>Department of Mechanical Engineering, University of Auckland, 20 Symonds St, Auckland, New Zealand

(Received March 30, 2015, Revised April 30, 2015, Accepted May 6, 2015)

**Abstract.** Climate changes brought on by human interventions have proved to be more devastating than predicted during the recent decades. Recognition of seriousness of the situation has led regulatory organisations to impose strict targets on allowable carbon dioxide emissions from automotive vehicles. As a possible solution, it has been proposed that Fibre Metal Laminate (FML) system is used to reduce the weight of future vehicles. To facilitate this investigation, FML based on steel and self-reinforced polypropylene was stamp formed into dome shapes under different blank holder forces (BHF) at room temperature and its forming behaviour analysed. An open-die configuration was used in a hydraulic press so that a 3D photogrammetric measurement system (ARAMIS) could capture real-time surface strains. This paper presents findings on strain evolutions at different points along and at 45° to fibre directions of circular FML blank, through various stages of forming. It was found initiation and rate of deformation varied with distance from the pole, that the mode of deformations range from biaxial stretching at the pole to drawing towards flange region, at decreasing magnitudes away from the pole in general. More uniform strain distribution was observed for the FML compared to that of plain steel and the most significant effects of BHF were its influence on forming depth and level of strain reached before failure.

**Keywords:** fibre metal laminate, real-time strain measurement system, self-reinforced polypropylene, stamp forming

### 1. Introduction

Current trend in the automotive industry is to replace traditional steel parts with advanced composite materials, to alleviate the growing anthropological impacts on the environment. With the aim of reducing carbon dioxide emissions from road vehicles which are identified as one of the largest contributors to global warming, ambitious targets have been imposed on automobile manufacturers by legislations worldwide. General response to this was to improve efficiency in performance of cars by using innovative technologies and reducing weight. Reduction in weight of the vehicles has been tackled by many companies by replacing traditional steel parts with fibre-

---

\*Corresponding author, Ph.D., E-mail: [shankar.kalyanasundaram@anu.edu.au](mailto:shankar.kalyanasundaram@anu.edu.au)

reinforced composites. From this, it has been suggested by several researchers that feasibility of use of an advanced hybrid material system called fibre metal laminate (FML) be investigated.

FML consists of alternating layers of metal and fibre-reinforced composite. It has advantages of lightweight and having improved impact and fatigue resistance while retaining high mechanical properties of the metal. FML has traditionally utilised thermosetting resins for the composite layers and was formed by a layup process. Although this does not pose a large hindrance for applications in the aerospace industry which it had originally been developed for, the high cost and time involved limit its use in mass production. To allow its employment in the automotive industry, researches have been launched previously on pre-consolidating FML panels using thermoplastic composite materials and subsequently processing it by stamp forming. (Compston *et al.* 2004, Mosse *et al.* 2005, Mosse *et al.* 2006a, b, Gresham *et al.* 2006, Sexton *et al.* 2012, Kalyanasundaram *et al.* 2013)

A composite based on thermoplastic matrix has the advantage over one based on thermosetting resin in that it can be formed under increased temperature at which the polymer becomes softer, and be cooled back, reobtaining its properties. This means that rather than having to be formed into its final product form like with thermoset, it can be pre-consolidated into sheets and be stamp formed afterwards when required, as was validated by Hou *et al.* (1994). This makes its mass production easier, as stamp forming is a method extensively used when a large number of parts has to be produced quickly under automation. In addition, thermoplastics are tougher and have higher impact resistance, as well as higher recyclability, making it an attractive option for use in automotive industry. An example can be seen in BMW i3 which had its production version released in 2013 and this vehicle has an outer skin made entirely of thermoplastic which has half the weight of steel, except for roof which is made out of CFRP (BMW Group 2014). High potential in use of thermoplastic-based composite was illustrated by Davey *et al.* (2013) as well, by investigating stamp forming of composite sheet based on carbon fibre and polyether ether ketone, which can exhibit strength higher than that of steel while being considerably more lightweight.

In past, researches have been carried out on stamp forming of FMLs, often with attention brought to effect of process parameters on formability of the material system. It was observed for draw forming of cups from FMLs consisting of aluminium and either glass-fibre-reinforced polypropylene (GFRP) or self-reinforced polypropylene (SRPP) wrinkle at low blank holder force (BHF) and under higher temperatures, while fracturing occurs at higher BHF's. (Mosse *et al.* 2005, Mosse *et al.* 2006a, b, Gresham *et al.* 2006) Forming limit curves based on mode of deformation for the FMLs were also suggested in attempt to establish limits on their manufacturability in the same way it has been developed for and used in traditional sheet metal forming (Sexton *et al.* 2012).

This paper investigates forming properties of steel/SRPP-based FMLs, in effort to benefit from the lightweight structure of an FML, superb forming qualities of steel and the ability of thermoplastic-based fibre-reinforced composite to be formed by stamp forming. This was done by analysing 3D strains at various stages of stamp forming of FML blanks at room temperature. BHF was also varied to investigate the effect of change in the process parameter on the formability of the material system.

## 2. Experimental procedures

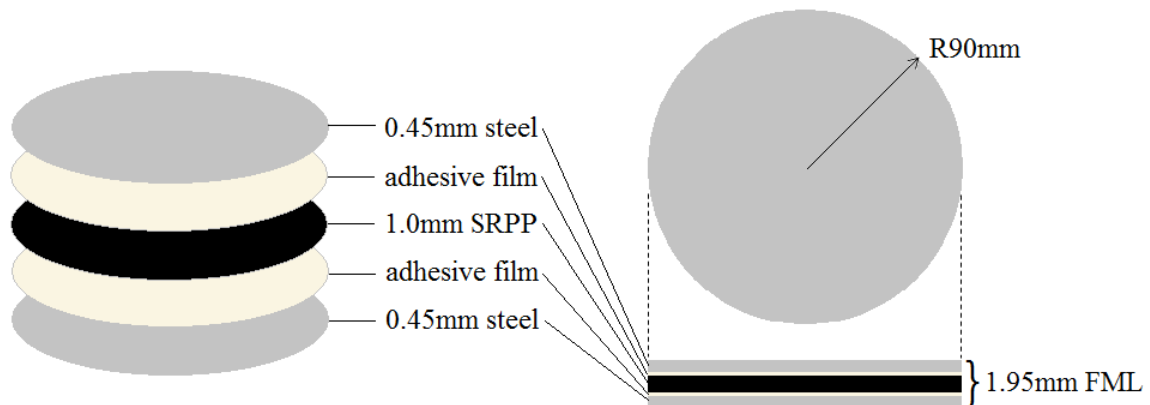


Fig. 1 Steel/SRPP FML blank layup and dimensions

### 2.1 Material and specimen preparation

FML specimens were made by bonding two steel sheets of 0.45 mm thickness each to either side of a 1.0 mm-thick SRPP sheet, using hot-melt film adhesives. (See Fig. 1.) Rectangular component layers were placed in a platen press at 145°C and held together with minimal pressure for 5 minutes to melt the adhesive films. The pressure on the laminate was then raised to 1.2 MPa and held for 5 minutes, ensuring good adhesion between the layers. Finally, the laminate was rapidly cooled to 35°C over the course of approximately 7 minutes to form a 1.95 mm-thick steel/SRPP FML. This was then cut into a circular blank with a diameter of 180 mm.

Curv<sup>®</sup> developed by Propex Fabrics was used for the SRPP. It is manufactured by hot compaction of polypropylene tapes which are extruded and then woven in a twill weave pattern. During hot compaction, surface of the polypropylene fibres are melted and recrystallised to form the matrix material. The resulting bidirectional composite is light-weight (0.9 g/cm<sup>3</sup>) and fully recyclable. For steel, GALVABOND<sup>®</sup> G2 from BlueScope Steel was used. It is hot-dipped zinc coated and is of commercial forming grade for general manufacturing, with density of 7.85 g/cm<sup>3</sup>. As for the adhesives, Collano 22.010, a thin film of thermoplastic based on modified polyolefines was used. It is made by Collano<sup>®</sup> and has a minimum bonding temperature of 130°C and density of 0.9 g/cm<sup>3</sup>. Stress-strain curves of the steel and SRPP are shown in Fig. 2.

### 2.2 Experimental setup

Forming experiments were conducted using a 300kN double-action mechanical press with hydraulic ram, fitted with an open die and a blank holder of 105 mm diameters and a 100 mm-diameter semi-hemispherical punch, as shown in Fig. 3(a). For lubrication, a thin sheet of polytetrafluoroethylene was placed between the punch and the circular blank. A blank was held by the blank holder at the flange region against the die and stamp formed into shape of a dome by the punch travelling at feed rate of 20 mm/s until maximum force had been reached in the load cell. BHF was varied to investigate its effect on forming, at 2 kN, 7 kN and 14 kN, and each test was repeated thrice.

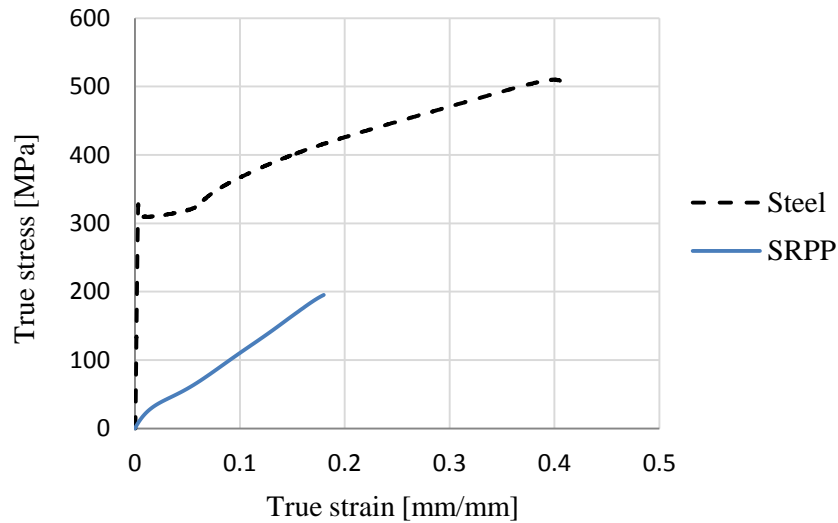


Fig. 2 Stress-strain curves of steel and SRPP along  $0^\circ/90^\circ$  fibre directions

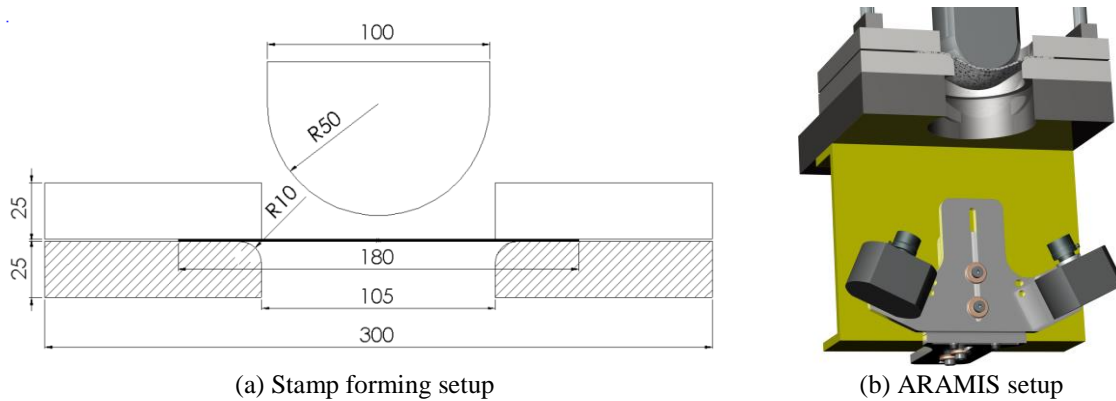


Fig. 3 Stamp forming experimental setup: (a) Cross section the punch, blank holder, blank and the die (Davey 2012), (b) positioning of ARAMIS cameras under the stamping press (Venkatesan 2012)

ARAMIS, a 3D photogrammetric measurement system developed by GOM mbH, was used to analyse surface strains on the part of the blank that is not obscured by the die. ARAMIS utilises two high resolution digital cameras which are placed beneath the die as shown in Fig. 3(b). Deformation of the blank is captured real-time by taking images at high speed, from which full-field strain of the blank can be computed based on 3D image correlation. This allows strains to be analysed at different stages of forming in various ways using the system's in-built software.

### 3. Results and analysis

#### 3.1 Wrinkling and delamination

Stamp formed steel/SRPP FML samples fail by wrinkling at the flange region held between the die and the blank holder. Although wrinkles increase in frequency with increase in BHF, amplitude and degree of propagation of wrinkles into the dome of the formed part are larger at lower BHFs. Hence, the severity of wrinkling is less pronounced at higher BHFs, which agrees with observations in past research on stamp forming of FMLs. However, at 14 kN BHF, delamination between the constitutive layers of the FML occur and partial delamination was seen in a specimen of a sample stamped with 7 kN BHF.

Wrinkling depth is defined in this paper as the maximum depth before wrinkling is detected in the blank at the edge of the die within the detectable range of ARAMIS cameras. It must be noted that the flange region is obscured by the die and cannot be analysed using ARAMIS. The largest wrinkling depth was observed with BHF of 7 kN and the lowest with 2 kN BHF. Wrinkling depths are shown in Table 1.

It could be seen by measuring diameters of the formed domes that the FMLs formed under 7 kN and 14 kN BHFs stretch slightly more along 45° meridian lines, where an  $x^\circ$  meridian line is defined as a straight line passing through the pole (centre of the blank) at  $x^\circ$  to the fibre directions in the SRPP layer, as shown in Fig. 4. This observation was more pronounced in the SRPP layer which also had more springback compared to the steel layers.

### 3.2 Strain evolution

There are several ways to study stamp forming behaviour of a material by analysing real-time surface strains. One way is to examine evolution of strains at different points on the blank as the forming process progresses. An example is shown in Fig. 5, where major and minor strains are plotted against time, showing evolution of strains through different depths, as an FML blank is

Table 1 Wrinkling depths FMLs stamped formed with different BHFs

Blank holder force [kN]	2	7	14
Wrinkling depth [mm]	17±5	37±2	33.8±0.6

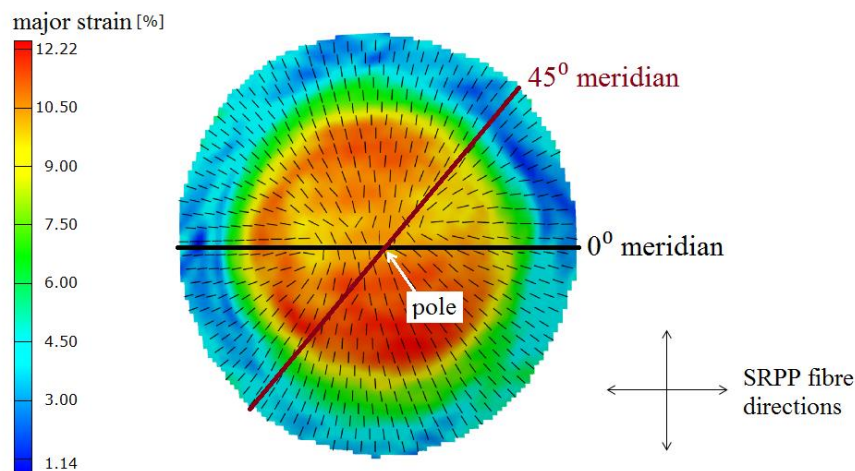


Fig. 4 Illustration of meridian lines used in analysis

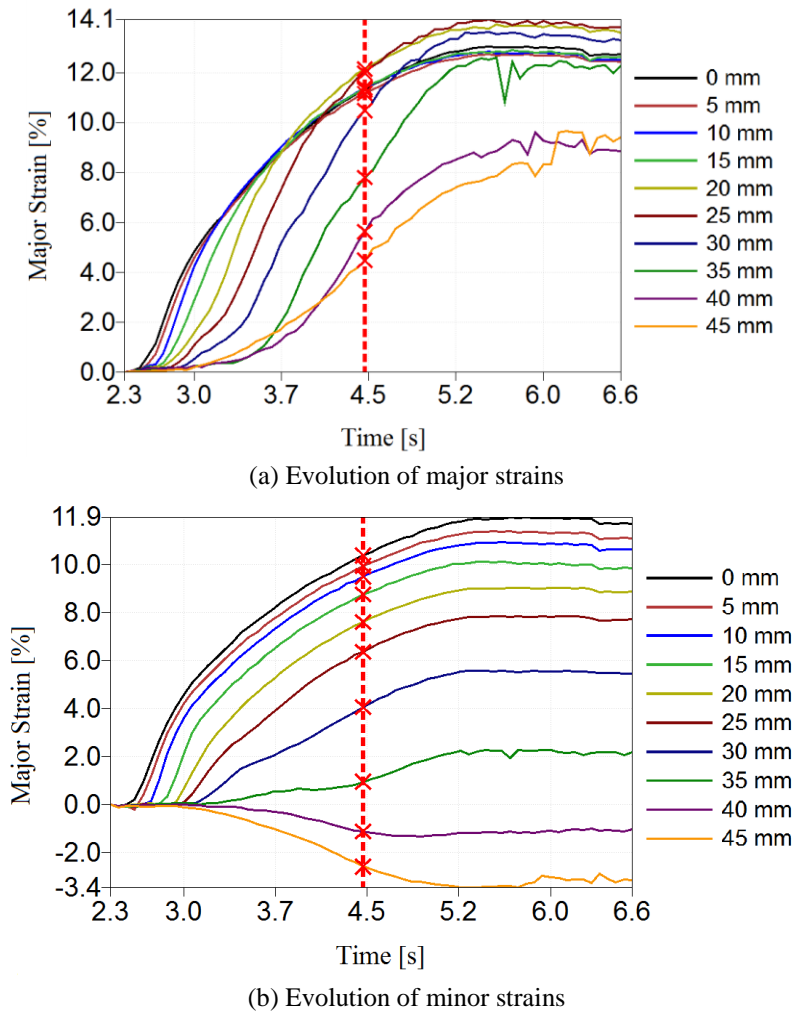


Fig. 5 (a) Major and (b) minor strains against time, at different points along  $0^\circ$  meridian of an FML stamp formed with 14 kN BHF. Time at which wrinkling occurs is shown by dotted lines

stamped under a 14 kN BHF. Strains were analysed at the pole and at several points along the  $0^\circ$  meridian, distanced 5 mm~45 mm from the pole at 5 mm increments. From observing evolution of major strains through different stages of forming (Fig. 5(a)), it can be seen that initiation of strain occurs at lower depths of forming at points closer to the pole between distances 0~30 mm from the pole, followed by the point nearest to flange area of the blank (45 mm from the pole), and then by points between these regions (35 mm and 40 mm from the pole). Similarly, minor strain (Fig. 5(b)) initiates starting from points closest to the pole except at 45mm which begins to strain at the same time as at 20 mm from the pole.

Paying attention to the rate at which strains develop at different points, major strains show an interesting behaviour. For points between 0~30 mm, rate of strain increases in such a way that points further away from the pole, which start to strain during later stages of forming, reach levels of strains that are higher or comparable to that of strain at the pole by the stage of wrinkling.

Table 2 Major and minor strains along 0° meridian at wrinkling stage of an FML stamp formed with 14kN BHF

Distance from pole [mm]	Major strain [%]	Minor strain [%]
0	10.6	9.66
5	10.4	9.25
10	10.7	8.85
15	10.7	8.07
20	11.2	6.89
25	10.8	5.67
30	8.63	3.30
35	6.24	0.681
40	3.56	-0.807
45	3.27	-1.95

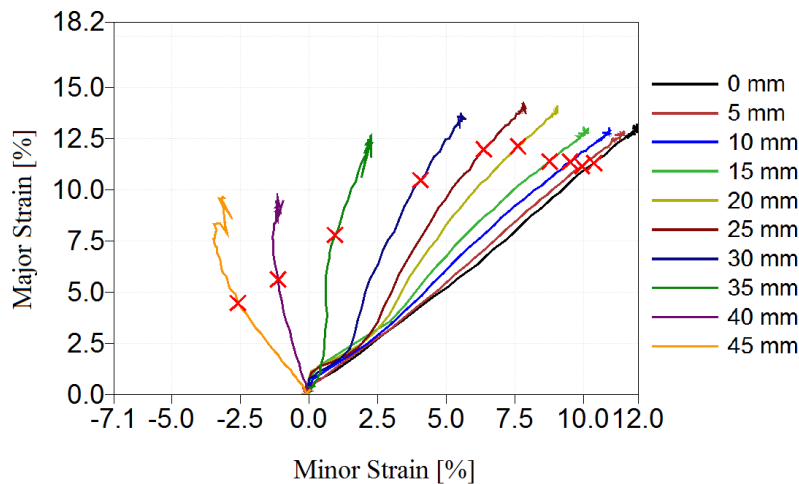
(Major and minor strains at the point of wrinkling are tabularised in Table 2 and shown as crosses where dotted lines indicating wrinkling stage intercept strain curves in Fig. 5). Similarly, the point closest to the flange strains at a lower rate, reaching a lower magnitude of strain at wrinkling depth than at points 35 mm and 40 mm from the pole, despite having started to strain at an earlier stage. Looking at the magnitude of strains at the final stage where maximum load has been reached, maximum major strains occur at points 20~30 mm, closely followed by points near the pole (0~15 mm), while minimum major strains occur near the flange, at 40~45 mm. Minor strains develop in a more simplistic pattern. At both wrinkling depth and maximum load, strains along the meridian decrease with distance from the pole, such that maximum strain occurs at the pole, zero strain occurs approximately 38 mm from the pole, and negative strain with increasing magnitude occurs towards the flange.

From the aforementioned observations, it can be gathered that the FML deforms starting from points on the blank which first come in contact with the punch, until at a certain depth, area closest to the flange where the material is restrained start to deform, followed by the region in-between. However, strains develop at different rates in different principal directions such that major strains increase slightly and then decrease with distance from the pole and minor strains progressively decrease in value with distance until it eventually becomes compressive towards the flange region.

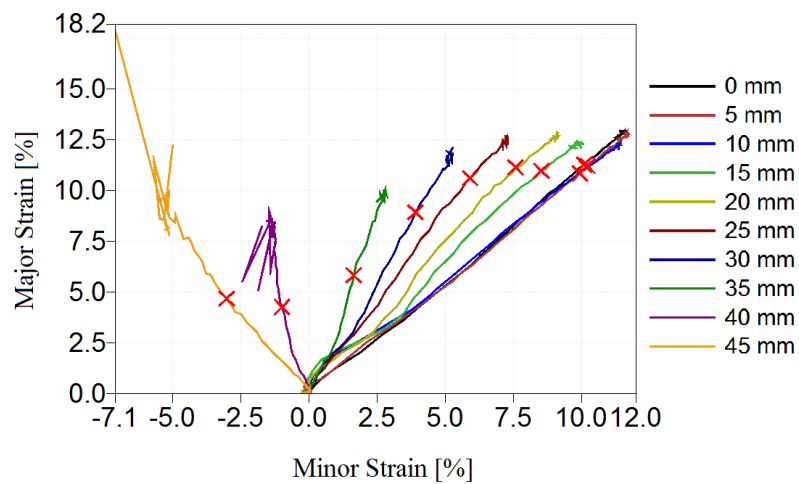
By combining the effect of both principal strains, it can be hypothesised that at wrinkling depth, the blank stretches biaxially at the pole, and as the distance from the pole increases, the material stretches more in one direction than the other until reaching a point at the side wall of the dome where it strains only in one direction (plane strain deformation mode). And finally, at regions closer to the die edge, it stretches in one direction but contracts in the other, leading to formation of wrinkling under localised buckling of the material in the flange region. Also, from studying magnitudes of the principal strains, it seems the amount of deformation by stretching decreases with distance from the pole in general.

This can be more or less be confirmed by plotting major strain against minor strain at the wrinkling depth, as in Fig. 6, from which different deformation modes at different points can be observed. Mode of deformation,  $\beta$ , is defined as ratio of minor strain to major strain and helps define forming properties of material for manufacturing (illustrated in Fig. 7). Observing deformation modes at different points along 0° meridian (Fig. 6(a), Table 3), there is a shift from

equal biaxial stretching ( $\beta=1$ ) at the pole through differing degrees of biaxial stretch ( $0<\beta<1$ ), plane strain deformation ( $\beta=0$ ) and uniaxial tension ( $\beta=-1/2$ ), reaching  $\beta\approx-0.6$  around edge of the die, just short of drawing ( $\beta=-1$ ). Although wrinkling is more likely in sheet metal forming where the mode of deformation exceeds beyond drawing ( $\beta=-1$ ) into uniaxial compression ( $\beta=-2$ ), this has not been observed in the FML blank at 45 mm from the pole, near the flange region. In considering this, it must be remembered that the flange region where the material actually wrinkles (50~90 mm from the pole) cannot be studied during forming, as it is held between the die and the blank holder. In terms of level of strains at stages of wrinkling and maximum load, magnitudes decrease with distance from the pole between 0~40 mm and increases slightly from 40 mm to 45 mm.



(a) 0° meridian



(b) 45° meridian

Fig. 6 Major strains against minor strains at different points along (a) 0° meridian and (b) 45° meridian of an FML stamp formed with 14kN BHF, until maximum load. Strains at wrinkling depth are marked with crosses

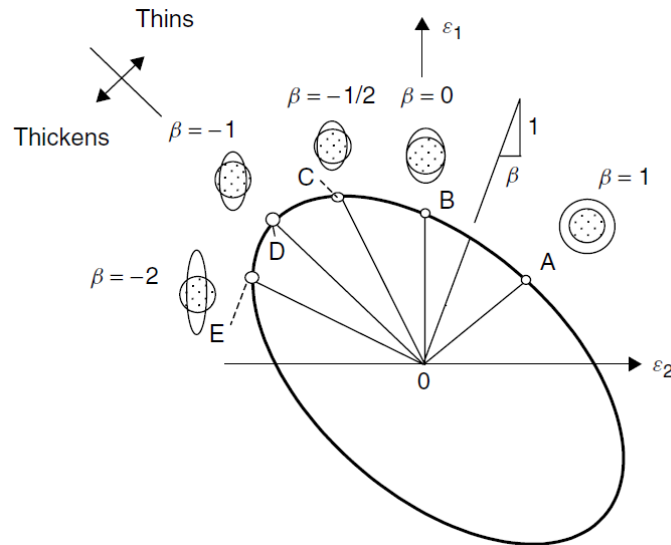


Fig. 7 The strain diagram showing the different deformation modes corresponding to different strain ratios. From right, equibiaxial stretching ( $\beta=1$ ), in plane strain ( $\beta=0$ ), uniaxial extension ( $\beta=-1/2$ ), drawing or pure shear ( $\beta=-1$ ) and uniaxial compression ( $\beta=-2$ ). (Marciniak 2002)

Table 3 Mode of deformation along 0° and 45° meridians during stamp forming of an FML with 14kN BHF

Approximate mode of deformation, $\beta$	Distance from pole, $x$ [mm]	
	Along 0° meridian	Along 45° meridian
unknown (likely $\beta < -0.6$ )	$45 < x \leq 90$	$45 < x \leq 90$
-0.6	45	45
0	37	38
$0 < \beta < 1$	$5 \leq x \leq 35$	$15 \leq x \leq 35$
0.9		$0 \leq x \leq 10$
1	0	

Effect of directionality of the SRPP layer propagating to the steel layer in the FML can be evaluated by plotting major strains against minor strains for points lying along a 45° meridian line, as shown in Fig. 6(b), and comparing with the plot drawn for strains along the 0° meridian line. Similar patterns are seen along the 45° meridian, in terms of variation in deformation modes (also shown in Table 3) and magnitude of strains with distance from the pole. However, few differences can be seen in comparing the magnitude of strains at the same distances along the two meridian lines. At both stages of wrinkling and maximum load, strains along the 45° meridian are smaller than those along the 0° meridian at points 15~40 mm from the pole and comparable or slightly larger at points 0~10 mm from the pole. Largest difference is observed at 45 mm from the pole, where the blank strains approximately to same extent before wrinkling but is significantly larger at maximum load along the 45° meridian. When major and minor strains along the 45° meridian are plotted against time, similar characteristics to 0° meridian can be seen, except that the major strain

continually decreases with distance from the pole, instead of showing a slight increase at the vicinity of the pole, followed by decrease towards the edge.

Summing these forming characteristics with the aforementioned observation that the material exhibited more stretch along  $45^\circ$  meridians, especially in the SRPP layer, it seems that the FML experiences larger overall elongation along the  $45^\circ$  meridian line because of the larger strain at and near the flange region compared to those along  $0^\circ/90^\circ$  meridians, and the slightly larger strain near the pole (0~10 mm) overcoming the smaller strains between 15~40 mm from the pole. This suggests that trellising occurred along the  $45^\circ$  meridians in the SRPP layer to a degree such that the effect was manifested in the steel layers through load transfer. (Trellising is a phenomenon where fibres in woven structures rotate under forces applied off-axis such that fibres are aligned more along the line of force and the resulting angles between weft and warp fibre directions are no longer at  $90^\circ$  to each other. The final result is that the material is sheared and stretched along the line of force.) It would also seem that the larger extensions around the pole and flange regions in the steel surface occur due to the shearing in the SRPP layer, to an extent that the amount of strain required in the region between the pole and the flange for total elongation (along the meridian) is reduced. In other words, either the amount of shear in the SRPP layer or the amount of load transfer to the steel layer is lower for some region between the pole and the flange area along  $45^\circ$  meridians. This hypothesis should be investigated by finite element analyses recommended for future research.

Similar difference in strains along  $0^\circ$  and  $45^\circ$  meridians can be observed in FMLs tested with 2 kN and 7 kN BHF, except for few differences: It is more pronounced at maximum load than at wrinkling stage when formed under 2 kN BHF, and with 7 kN BHF, the FML has larger strain near the flange along  $45^\circ$  meridian than along  $0^\circ$  meridian at stages of both wrinkling and maximum load.

Comparison between forming properties of plain steel and steel/SRPP FML can be made by looking at Fig. 8, showing graphs of major strains against minor strains along fibre directions

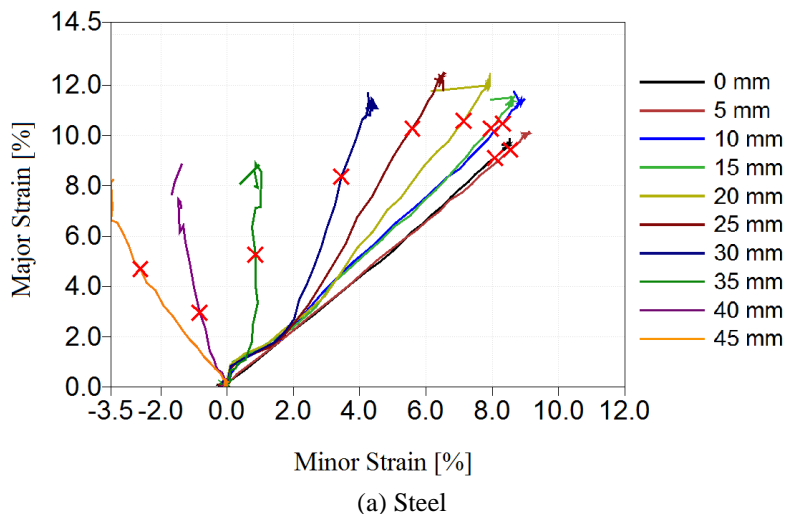


Fig. 8 Graphs of major strains against minor strains at different points along  $0^\circ$  meridians of (a) steel and (b) FML samples stamp formed with 14 kN BHF, until maximum load. Strains at forming depth of 30 mm are marked with crosses

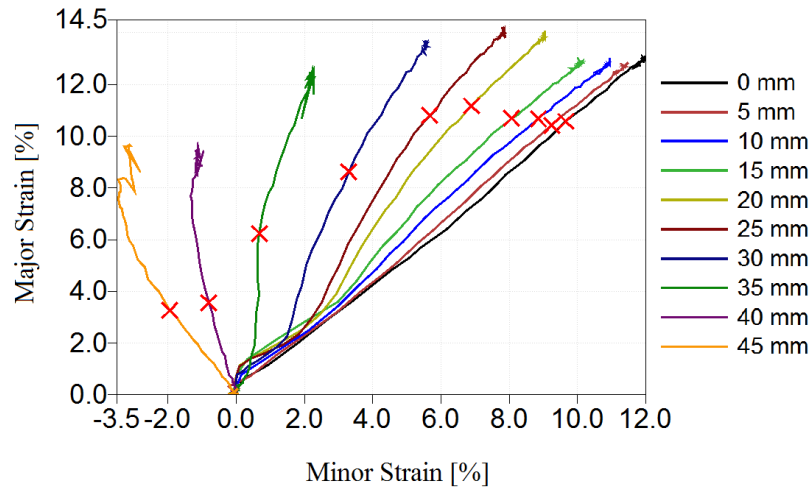


Fig. 8 Continued

when formed under 14 kN BHF. Strain distribution of steel compares to that of the FML in that it has larger degree of variation along the  $0^\circ$  meridian, where the strain increases with distance from the pole and then decreases to quite a low value between 35~40 mm and then increases again at the edge. The uniformity in strain distribution of the FML can be advantageous in that it may provide stability and predictability in the metal layer from failure by necking. However, it must be kept in mind that the SRPP and inner steel layers could not be observed for these experiments and that wrinkling and delamination are failure mechanisms which require more immediate attention, in these instances.

Effect of forming with different BHFs was also investigated, with results shown in Fig. 9. From the graphs of major strains against minor strains, a general increasing trend in the magnitude of strains at maximum load is observable for increase in BHFs. However, further investigations show that strains are comparable (although not the same) at similar depths despite the difference in BHFs, and it seems the most significant effect of BHF is difference in forming depths and therefore strains it allows the material to undergo before wrinkling. Overall magnitude of strain at wrinkling stage is the lowest for FML stamped with 2kN and comparable but slightly higher for 7 kN than 14 kN, which corresponds to the trend in the wrinkling depth. An interesting point to pay attention to is the difference in magnitude of strains at wrinkling compared to maximum load, depending on the BHF. For example, similar depths and therefore the level of strains are achieved just before wrinkling using BHFs of 7 kN and 14 kN, and yet, the FML blank stamped with 14 kN BHF strains much further after wrinkling until maximum load is reached. From this, it can be hypothesised that there is more potential for the forming limit to be improved using 14 kN BHF if wrinkling and delamination (which may be related to one another) can be controlled, for example, by varying other parameters such as forming temperature. Further future research is suggested for verification.

From the graphs of major strains against minor strains in Fig. 9, an interesting behaviour can be observed. At different points along the blank, the material undergoes a change in deformation mode at different depths, marked by a noticeable change in the gradient. For example, in Fig. 9(c),

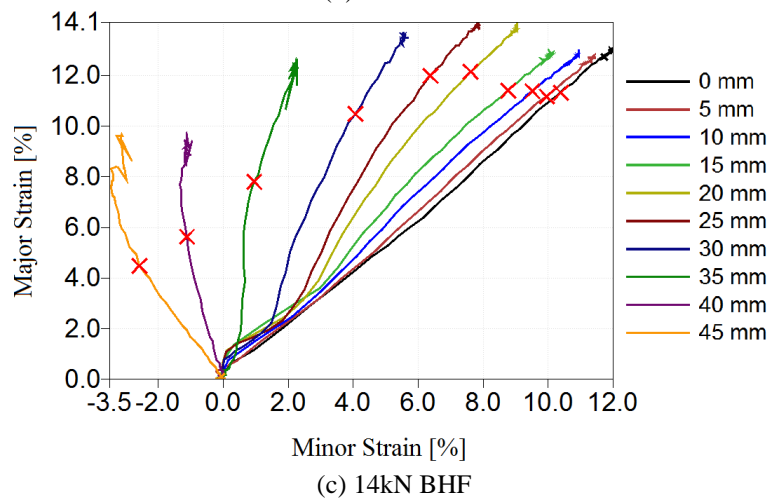
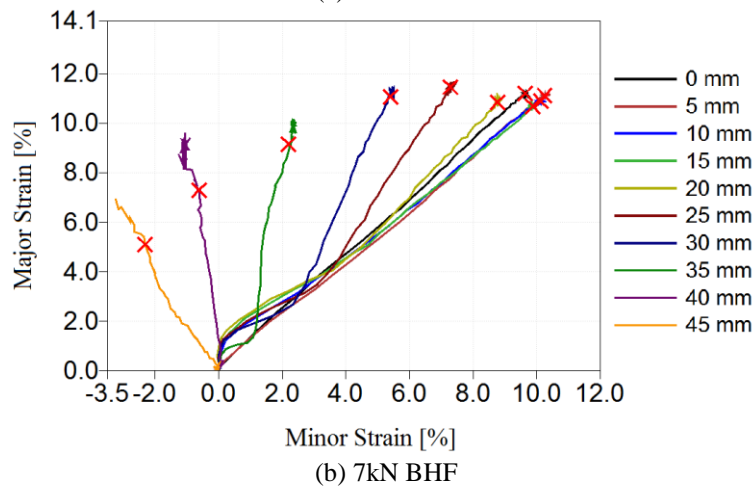
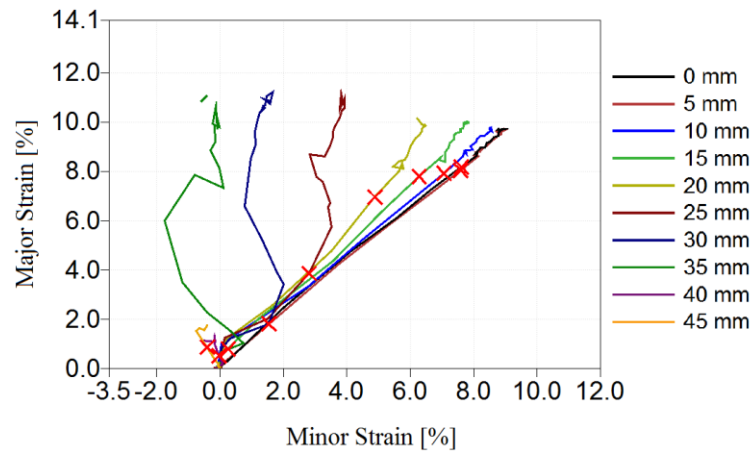


Fig. 9 Major strains plotted against minor strains at different points along  $0^{\circ}$  meridians of FML samples stamp formed with a) 2kN, b) 7kN and c) 14kN BHF, until maximum load. Strains at wrinkling depth are marked with crosses

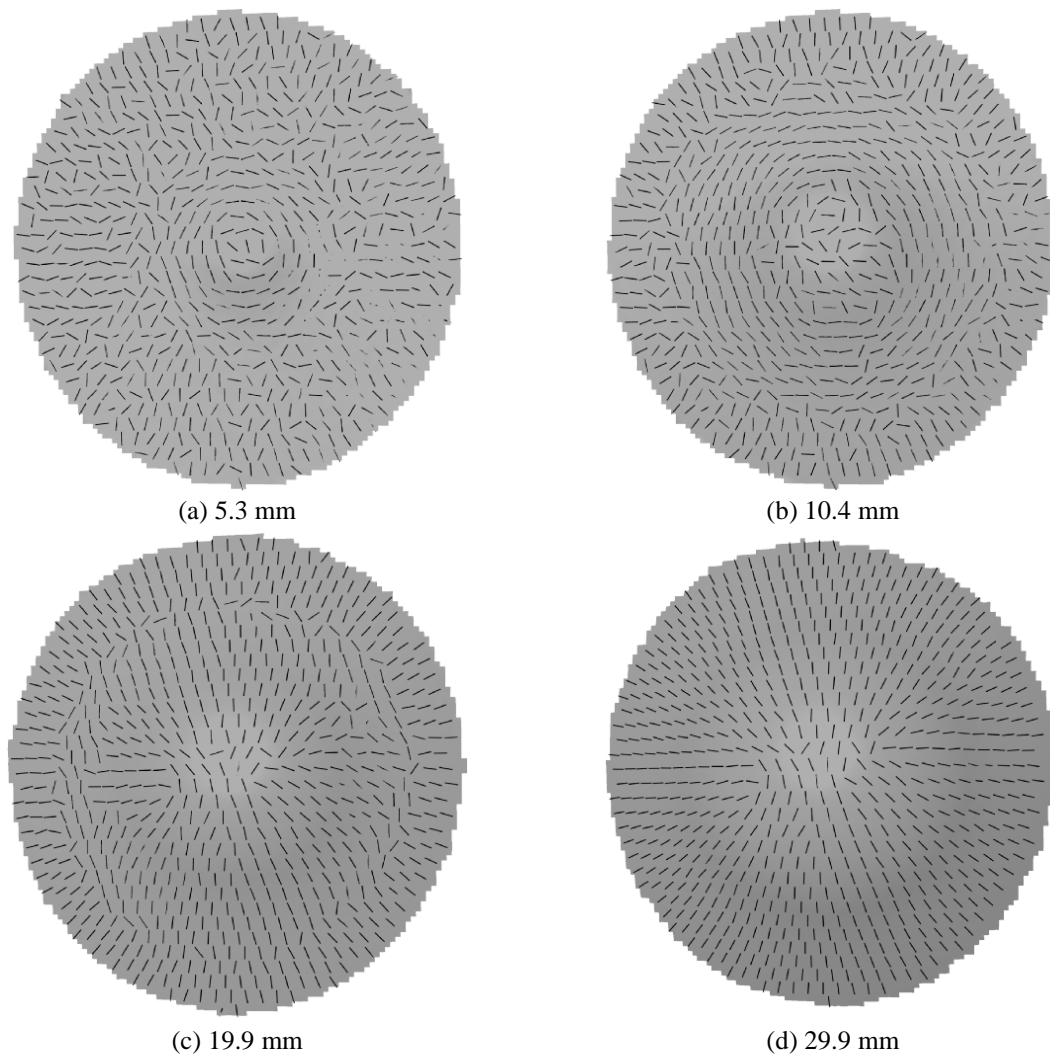


Fig. 10 Direction of major strains shown as lines distributed over the FML specimen stamp formed with 14 kN BHF, at depths of (a) 5.3 mm, (b) 10.4 mm, (c) 19.9 mm and (d) 29.9 mm

this occurs at the pole and 5 mm point when the major strain is just below 0.5%, at points 15~25 mm from the pole at approximately 1% major strain, and at 35 mm from the pole when the major strain reaches around 7.5%. Studying the direction of major and minor strains at different stages of forming reveals that this is not merely a change in the rate at which the magnitude of strains grow in respective principal directions, but a swap in principal strain directions.

This is illustrated in Fig. 10, where direction of major strains are shown as lines distributed over the surface of on an FML blank, at different stages of forming. For instance, during early stages of forming where the forming depth is low, major strains occur along tangential directions to the meridian lines in the region around the pole (Fig. 10(a)). As forming progresses, more material in the region between the punch and the die where the blank is not in contact with any tool deform such that largest strain occur tangentially (Fig. 10(b)). As forming depth increases,

material strains more prominently in radial directions than in tangential directions (swap in first and second principal directions), where this change starts near the pole and moves outwards (Fig. 10(c)), until the blank is deforming most significantly in radial directions, i.e., major strains are radial (Fig. 10(d)). This swap over of major and minor strain directions occur within 40 mm radius of the pole. At approximately 40 mm from the pole, deformation occurs in plane strain mode, straining only in radial direction, and beyond this, the outer region of the blank also has major strains in radial directions as these experience negative minor strains in tangential directions. This phenomenon is also reflected in Fig. 9(c) where at points 40 mm and 45 mm from the pole, for which the curves do not show the sudden change in the gradient.

It may be visualised that the blank initially strains more in tangential directions as the punch makes contact with the blank, and then strains more extensively in radial directions subsequently with more material flow permitted inwards from the edges, as the punch force overcomes the friction between the material and the tool and the blank gets drawn into the die.

### **3. Conclusions**

Stamp forming behaviour of steel/SRPP FML has been investigated at room temperature under BHF of 2 kN, 7 kN and 14 kN. Failure occurred in the laminate system by wrinkling after which maximum load was reached at a larger depth. Severity of wrinkles decreased with increasing BHF but delamination between layers were observed for a sample formed with BHF of 14 kN, and partial delamination occurred in a specimen formed with 7 kN BHF. By observing 3D surface strains at different points on the blank and analysing how they evolve through different stages of forming, it could be gathered that deformation begins at the pole and moves to surrounding regions, as the punch makes contact with the blank. Strains occur to a larger extent initially in tangential directions and then in directions pointing towards the pole.

It was evident that different regions of the blank deform under different deformation modes, ranging from biaxial stretching in the centre to uniaxial tension and drawing towards the flange region. At stages of wrinkling and maximum load, magnitudes of strains generally decrease with distance from the pole along  $0^\circ$  meridians. Along  $45^\circ$  meridians, slightly different strain distribution is observed in terms of magnitude, exhibiting some degree of directionality due to the presence of fibre orientations in the SRPP layer. More uniform strain distribution is achieved by using FML compared to plain steel which may translate to better forming characteristics. This requires verification by further investigation.

Comparing use of different BHFs, it was found that it controls the depth the blank could be formed to prior to wrinkling, which is closely related to the level of strain developed in the material. The largest wrinkling depth was observed at 7 kN BHF, meaning that most strain occurred in specimens formed with this BHF. However, 14 kN BHF sample could be formed to a depth and strains very close to that of 7 kN BHF, while experiencing larger strain up to maximum load, suggesting that forming limits of the FML may be improved if wrinkling and delamination can be more carefully controlled via other process parameters.

It is therefore suggested that further research is carried out on varying process parameters. This includes use of lock ring (s) to increase blank holding force which may suppress wrinkling but increase of which is limited by the machine specifications. It is also recommended that experiments be repeated at higher temperatures so as to induce different forming behaviours of SRPP. This would allow closer investigation of forming characteristics of the FML and optimal

forming condition can be suggested with regards to forming limits. As to earlier speculation on whether more uniform distribution induced by addition of SRPP to plain steel results in better formability, aforementioned further research would give insight to the hypothesis as it is yet too early to give a precise conclusion on the matter without further data. Furthermore, some of the crucial information we lack for deciphering forming behaviours of the FML system are deformations through the thickness of the materials and within the SRPP layer. This is why finite element modelling is recommended for more in-depth study of forming properties of the steel/SRPP FML, to allow analyses on parts which cannot be observed or measured during the forming procedure.

## References

- BMW Group, "Lightweight and robust, the thermoplastic outer skin", BMW Group, viewed 18 July 2014, [http://www.bmwgroup.com/e/0\\_0\\_www\\_bmwgroup\\_com/produktion/BMW\\_I/aussenhaut\\_des\\_BMW\\_i.html](http://www.bmwgroup.com/e/0_0_www_bmwgroup_com/produktion/BMW_I/aussenhaut_des_BMW_i.html).
- Compston, P., Cantwell, W.J., Cardew-Hall, M.J., Kalyanasundaram, S. and Mosse, L. (2004), "Comparison of surface strain for stamp formed aluminum and an aluminum-polypropylene laminate", *J. Mater. Sci.*, **39**, 6087-6088.
- Davey, S. (2012), "Investigation into the formability of carbon fibre/polyester ether ketone composite sheets in stamp forming processes", *15<sup>th</sup> European Conference on Composite Materials (ECCM15)*, Venice, June.
- Davey, S., Das, R., Cantwell, W.J. and Kalyanasundaram, S. (2013), "Forming studies of carbon fibre composite sheets in dome forming processes", *Compos. Struct.*, **97**, 310-316.
- Gresham, J., Cantwell, W.J., Cardew-Hall, M.J., Compston, P. and Kalyanasundaram, S. (2006), "Drawing behaviour of metal-composite sandwich structures", *Compos. Struct.*, **75**, 305-312.
- Hou, M. and Friedrich, K. (1994), "3-D Stamp Forming of Thermoplastic Matrix Composites", *Appl. Compos. Mater.*, **1**, 135-153.
- Kalyanasundaram, S., DharMalingam, S., Venkatesan, S. and Sexton, A. (2013), "Effect of process parameters during forming of self reinforced-PP based fiber metal laminate", *Compos. Struct.*, **97**, 332-337.
- Marciniak, Z., Duncan, J.L. and Hu, S.J. (2002), *Mechanics of Sheet Metal Forming*, Butterworth-Heinemann, Oxford, UK.
- Mosse, L., Compston, P., Cantwell, W.J., Cardew-Hall, M.J. and Kalyanasundaram, S. (2005), "The effect of process temperature on the formability of polypropylene based fibre-metal laminates", *Compos. Part A*, **36**, 1158-1166.
- Mosse, L., Compston, P., Cantwell, W.J., Cardew-Hall, M.J. and Kalyanasundaram, S. (2006), "Stamp forming of polypropylene based fibre-metal laminates: The effect of process variables on formability", *J. Mater. Pr. Tech.*, **172**, 163-168.
- Mosse, L., Compston, P., Cantwell, W.J., Cardew-Hall, M.J. and Kalyanasundaram, S. (2006), "The development of a finite element model for simulating the stamp forming of fibre-metal, laminates", *Compos. Struct.*, **75**, 298-304.
- Sexton, A., Cantwell, W.J. and Kalyanasundaram, S. (2012), "Stretch forming studies on a fibre metal laminate based on a self-reinforcing polypropylene composite", *Compos. Struct.*, **94**, 431-437.
- Venkatesan, S. (2012), "Stamp forming of composite materials: an experimental and analytical study", Ph.D. Dissertation, Australian National University, Canberra.